Journal of
Materials Chemistry C

Materials for optical, magnetic and electronic devices
www.rsc.org/MaterialsC

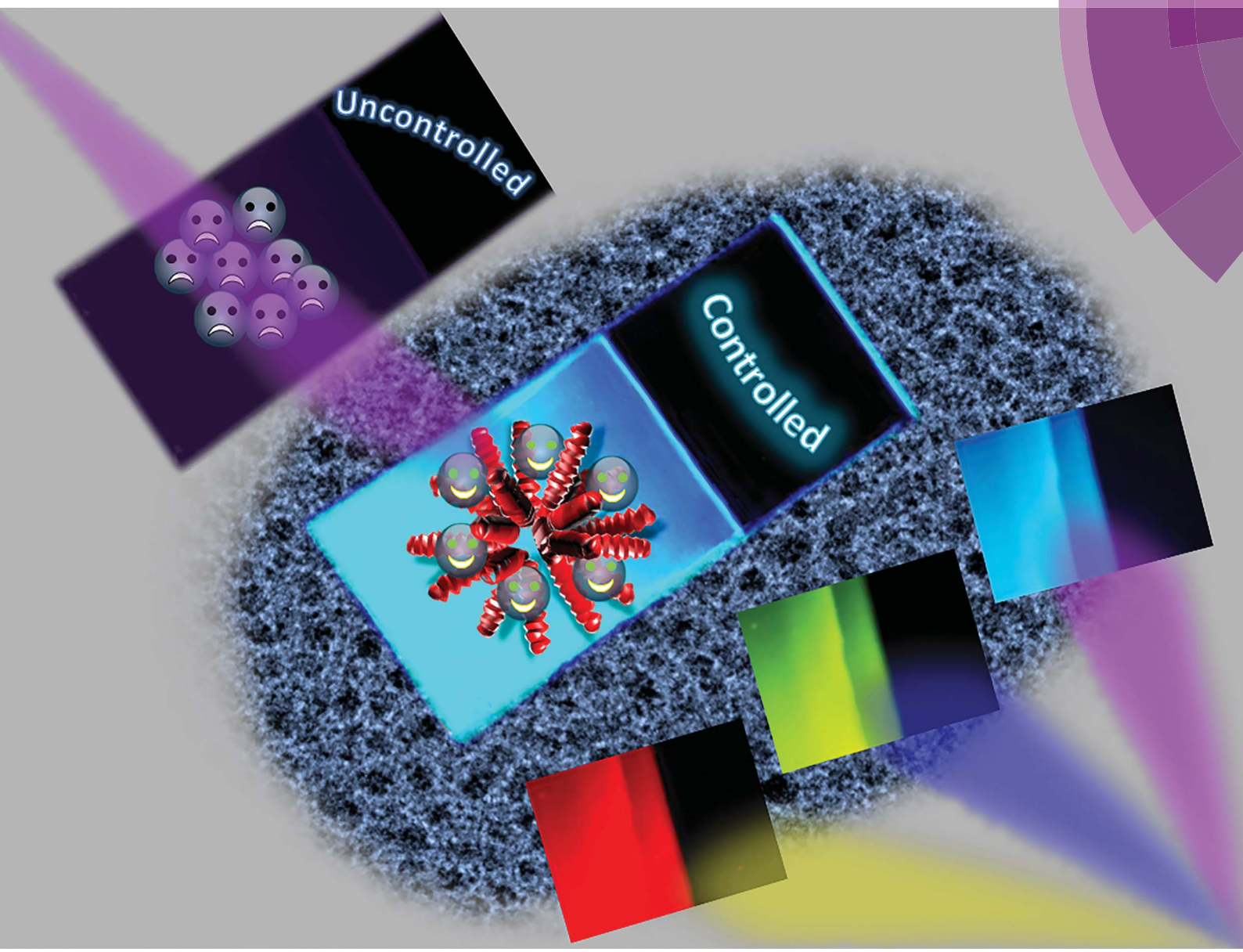

ISSN 2050-7526

ROYAL SOCIETY OF CHEMISTRY

COMMUNICATION
Goutam De *et al.*
Carbon nanodot–ORMOSIL fluorescent paint and films

Journal of Materials Chemistry C

COMMUNICATION

View Article Online
View Journal | View Issue

Cite this: J. Mater. Chem. C, 2015, 3, 714

Received 22nd September 2014
Accepted 2nd November 2014

DOI: 10.1039/c4tc02140a

www.rsc.org/MaterialsC

Carbon nanodot–ORMOSIL fluorescent paint and films†

Manish Kr Mishra, Amrita Chakravarty, Koushik Bhowmik and Goutam De*

Controlled carbonisation of P123 block-*co*-polymer in ethanol yielded micelle-protected carbon nanodots (CNDs) at room temperature. A purified and concentrated CND solution (quantum yield 10%) was incorporated into the organically-modified SiO_2 (ORMOSIL) sol for the fabrication of transparent fluorescent coatings of thickness ~3 μm on glass. These films are scratch resistant with a surface hardness value of 8H. The sol can also be useful as a fluorescent ink/paint. The films retained the pristine photophysical properties of CNDs.

For the past many decades, cadmium- and zinc-based luminescent quantum dots (QDs) have dictated numerous applications in fields such as bio-imaging, LEDs, *etc.* due to their intense and tunable fluorescence.[1–4] They are very advantageous compared to conventional organic dyes in terms of their photostability and less overlapping absorption–emission spectra. However, most of these QDs or their precursors have significant toxicity[5–8] and require relatively high temperatures (150–300 °C) for solution phase synthesis.[9,10] Hence, non-toxic alternative fluorescent QDs are required to replace the traditional semiconductor QDs. Recently, fluorescent carbon dots have emerged as eligible candidates to take the place of semiconductor QDs due to their numerous advantages, including high photostability,[11] emission tunability,[11–13] water solubility[14] and potential for use as optical imaging tools.[13,15,16] Many research groups have synthesised CNDs *via* different techniques[17,18] and explored their exciting properties, such as their different emission colours,[17] powerful energy transfer components in photocatalysis,[12,14] and so on. Most of these synthesis methods involve carbonisation of a carbohydrate (glucose and sucrose) or polyethylene glycol by thermal or microwave treatment. However, these methods yielded a very broad particle size distribution and low quantum yield. Further, fluorescent CNDs are restricted to the solution phase (mainly in aqueous medium) and need attention on their availability in the form of thin films. Moreover, the retention of the primitive photoluminescence (PL) of CNDs in the presence of either electron donor or acceptor molecules is a challenging task as CNDs are excellent electron donors and acceptors themselves, resulting in significant PL quenching.[14] Also, recently Zeng *et al.* reported CND/polyvinyl pyrrolidone and CND/polyacrylic acid polymer composite films with very bright fluorescence.[19] However, the original emission of bare CNDs was lost in the polymer matrices. It is also noteworthy that organic polymer supports have poor adhesion properties and their hygroscopic nature slowly degrades the quality of film.[20–23]

Hence, solid supports such as dielectric matrices or films are essential for the confinement of fluorescent CNDs for optical applications.[24,25] Key points while selecting the support film matrix must be that it should not undergo an e^- donor–acceptor process with light emitting CNDs and prevent them from agglomeration. We found that organically modified silica, known as ORMOSIL,[26] is the best candidate for the stabilisation of CNDs in a hard and transparent nanocomposite film matrix. ORMOSIL can stabilise these CNDs from agglomeration and provide substantial spatial distribution throughout the film matrix due to the unavailability of a sufficient fluid environment (which restricts the individual particles from meeting each other *via* diffusion).[27] Besides these, it can also be used to produce hard adhesive films on glass and flexible plastic substrates. Very recently Zhang *et al.*[28] synthesised organosilane-functionalised CNDs, which can be used for coating on different substrates, but the synthesis method required a relatively very high temperature (240 °C) and generally this kind of amino silane forms very thin films with low surface hardness.

Keeping the above key points in mind we synthesised highly fluorescent CNDs from block-*co*-polymer P123 in EtOH (see Fig. 1a and b) and stabilised them in ORMOSIL sol, which has been used for the fabrication of scratch-resistant eco-friendly fluorescent coatings on glass (see Fig. 1c) and as a fluorescent

Nano-Stuctured Materials Division, CSIR-Central Glass & Ceramic Research Institute, 196, Raja S.C. Mullick Road, Kolkata-700032, India. E-mail: gde@cgcri.res.in

† Electronic supplementary information (ESI) available: Experimental and characterization (QY calculations, sample photographs, profilometeric trace, FESEM images, FTIR, SAXS, XRD, Raman spectra, UV-visible, PL spectra, Fig. S1–9 and Tables S1 and S2). See DOI: 10.1039/c4tc02140a

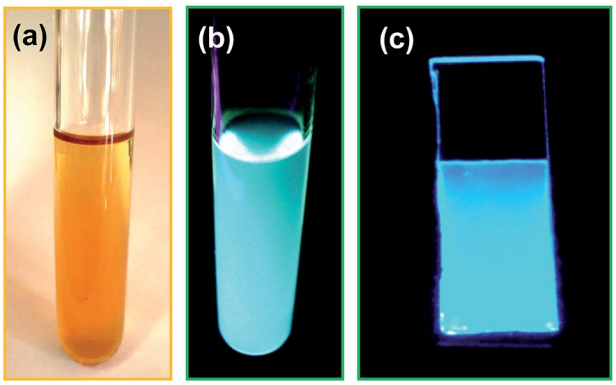

Fig. 1 Digital images of CNDs in ethanol solution under (a) normal light, (b) UV light and (c) corresponding CND-incorporated ORMOSIL film on glass under a UV lamp (λ_{ex} = 365 nm).

paint (see Fig. S1; ESI†). It is noteworthy that when the CNDs were added to sol–gel derived TiO_2 or ZrO_2 sol, no fluorescence was observed after film fabrication, which may be due to electron transfer between CNDs and TiO_2 or ZrO_2.

The P123 polymer was carbonised using concentrated H_2SO_4, followed by neutralisation by NH_3. The process yielded acid (–COOH) functionalized CNDs and the salt of the strong acid and weak base $(NH_4)_2SO_4$. Unwanted salt and excess P123 were removed by repetitive solvent (*n*-hexane : water 3 : 1 v : v) extraction. To achieve better stability (dispersibility) of CNDs, P123 was carbonised in such a way that some of the P123 chains remained undecomposed and could form micelles in EtOH solution,[29] as shown in the schematic diagram Fig. 2. These micelles stabilise the CNDs *via* hydrophilic–hydrophilic interactions between the CND surface and micelle exterior (PEO units).[30] Extra pure CNDs were obtained by column chromatography with silica gel as the stationary phase and *n*-hexane–ethyl acetate (99 : 1 v : v) as the mobile phase. Using this approach, 0.12 g of CNDs can be obtained from 1 g of P123 starting material. For the film fabrication process, the required amount of CNDs, obtained after solvent extraction (in *n*-hexane) or column chromatography (in *n*-hexane–ethyl acetate 99 : 1 v : v), was concentrated to dryness (on a rotary evaporator) and mixed with ORMOSIL sol. The homogeneous sol obtained was used for dip-coating on glass and was cured at 70 °C for 6 h. The detailed experimental procedure is given in the ESI.† CNDs obtained from column chromatography were mainly used for the fabrication of durable and stable CND–ORMOSIL films, due to the lower contribution of undissociated P123 polymer present on the CND surface. ORMOSIL sol-originated terminal silanol (Si–OH) groups condensed with the surface OH groups of the glass substrate to produce a durable adhesive coating. The thickness of the CND–ORMOSIL film deposited on the glass substrate was measured by a profilometer and found to be ~3 μm (Fig. S2; ESI†). A similar thickness value was also observed by cross-sectional FESEM analysis (Fig. S3a; ESI†). The FESEM top view (Fig. S3b; ESI†) of the film showed a uniform and crack-free surface. Adhesion of the films on glass substrates was evaluated using the cross-cut tape test (ASTM D3359).[26] After the test, no peeling off of the films from the substrate was observed and the edges of the cuts were found to be completely smooth. Accordingly, the adhesion quality can be classified as 5B (highest quality). The surface hardness (using ASTM D3363 specifications) value of the CND–ORMOSIL film on glass was found to be 8H (ASTM 03363), which is quite high for any practical applications. Ellipsometric measurement of the CND–ORMOSIL film showed a refractive index of 1.489 at the wavelength of 633 nm.

The physicochemical properties of the CNDs were studied using FTIR, UV-visible and Raman spectroscopy, PL and PL decay lifetime measurements, fluorescence microscopy, TEM, XRD and SAXS analysis. Detailed FTIR analysis was done at different stages of the synthesis to understand the CND formation mechanism and the presence of any functional groups on the CND surface (Fig. S4; ESI†). It was observed that after carbonisation of P123 by H_2SO_4, followed by neutralisation with NH_3, the peak corresponding to C–O–C started obviously decreasing. This is due to the breakage of the C–O–C bond with the formation of CND particles. Also, prominent peaks corresponding to $-COO^-NH_4^+$ and $(NH_4)_2SO_4$ were observed near 1645 and 1106 cm^{-1}, respectively.[31] The peak at 1645 cm^{-1} (C=O of $COO^-NH_4^+$) red shifted to 1735 cm^{-1} after solvent extraction (using a *n*-hexane : water mixture, 3 : 1 v : v), which indicates that the $-COO^-NH_4^+$ was hydrolysed in the presence of water, forming –COOH and NH_4OH. Also, the excess unreacted P123 was separated (in the water phase) after solvent extraction, leaving behind some P123 that strongly interacted with the surfaces of the CNDs (in the hexane phase) *via* hydrophilic–hydrophilic interactions. The extraction was repeated 4 times by separating the *n*-hexane phase and the addition of fresh water (maintaining the same ratio of *n*-hexane and water), for the complete removal of $(NH_4)_2SO_4$ and the hydrolysis products of the $-COO^-NH_4^+$ group. Fig. S5 (ESI†) shows a digital picture of the CNDs (after solvent extraction 4 times) under room and UV light (365 nm). During the first cycle of extraction it was observed that some CNDs were transferred in the water phase, due to the presence of a large number of –COOH groups on them, which increased their polarity. To acquire extra-pure CNDs we performed column chromatography using SiO_2 as the stationary phase and *n*-hexane–ethyl acetate (99 : 1 v : v) as the mobile phase. The column-extracted product showed removal of almost all of the C–O–C band in the FTIR spectrum (Fig. S4; ESI†), suggesting that the hydrophilic SiO_2 surface kept them in column. An interesting point is that the peak corresponding to the acid groups remained the same even after repetitive solvent extractions and column, revealing the fact that this group is covalently attached to the CND surface, otherwise it would have been removed.

For particle size analysis, small angle X-ray scattering (SAXS) was performed (using Rigaku Nanosolver software) in transmission mode and the average particle diameter was found to be 3.5 nm (Fig. S6a; ESI†). Besides this, the high angle XRD pattern (Fig. S6b; ESI†) showed 3 broad peaks around 13.8°, 19°and 42° 2θ. The appearance of peaks at 13.8° and 42° corresponds to the oxidised graphite-like nature of the CNDs, with large interlayer spacing (d = 0.64 nm). Previously, Hu

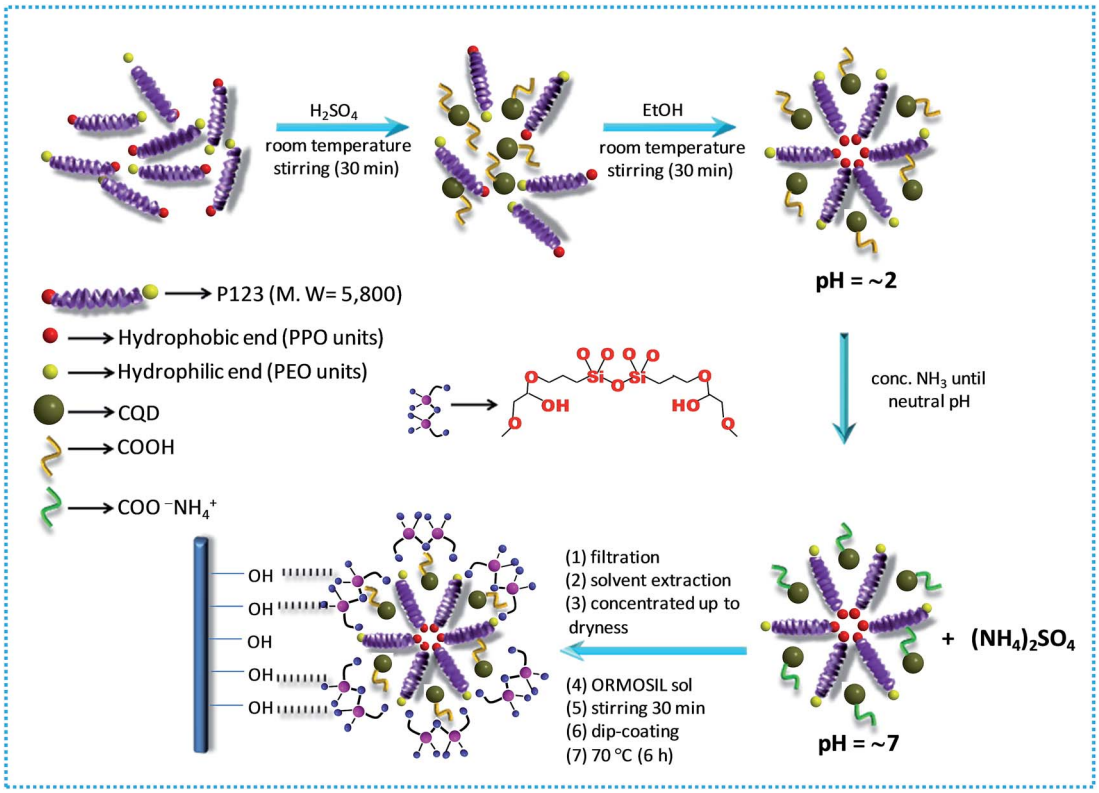

Fig. 2 Schematic diagram showing the mechanism of the CND synthesis.

et al.[32] and Aksay *et al.*[33] reported that the interlayer spacing of graphitic oxide is dependent on the amount of water (intercalated) and oxygen-containing groups (such as –OH, –COOH, epoxy) present in the system. They showed that with varying the time of acid functionalization (of graphite) or heating temperature (of graphitic oxide) the *d*-value can be tuned in the range of 0.756–0.337 nm, due to intercalation of functional groups or residuals. The peak near 19–20° 2θ is expected to be due to the amorphous nature of the matrix film.

TEM analysis of the purified CNDs showed well-dispersed spherical particles (Fig. 3a and b). The inset in Fig 3a shows the SAED pattern with a diffused ring pattern for the (002) and (001) planes, corresponding to 0.64 and 0.21 nm *d*-values. The insets of Fig. 3b show the particle size distribution (upper right) calculated from the TEM image and HRTEM image of one CND (lower left). An average CND particle size was found to be around 3.5 nm, which is similar to the value obtained by transmission SAXS analysis in solution. The hazy fringe pattern of the CND, as observed from the HRTEM (Fig. 3b, inset), gives an indication that the CNDs are poorly crystalline. TEM of the corresponding CNDs in the ORMOSIL matrix is also shown in Fig. 3c and d. This shows the presence of uniform and agglomeration-free CNDs, as observed in the case of CNDs in solution. Thus, SAXS and TEM analysis confirmed uniform distribution of CNDs in solution as well as in the ORMOSIL film matrix. Micro-Raman analysis showed that the synthesised CNDs have an oxidised graphite-like structure with substantial defects. Fig. S7 (ESI†) shows the Raman spectrum of bare CNDs and the peaks around 1610 and 1306 cm^{-1} exhibit the signature of a highly functionalised graphite-like structure.

The blue shift of the G-band to 1610 cm^{-1} is due to the overlapping of the G- and D′-bands, which is a characteristic feature of oxidised graphite.[34] Further, the broadness of the peaks, with much higher relative intensity of the D-band compared to the G-band ($I_D/I_G = 1.25$), confirms the functionalised nature of the CNDs, with defects similar to those in graphite oxide, in accordance with XRD results.[35]

Preliminary indication of CND formation was observed by UV-visible spectroscopy, which showed a well-resolved absorption peak at around 300 nm, with a long absorption edge (Fig. S8a; ESI†). This absorption property remained unchanged in the case of the CND–ORMOSIL film (see the inset of Fig. 4) and the result indicates the similar nature of dispersed CNDs in the film matrix as well. The appearance of a long tail in the UV-visible spectrum indicates some size distribution of the CNDs. PL spectra of bare CNDs showed an excitation (305–525 nm) dependent emission property in the wavelength range of 350–650 nm (Fig. S8b; ESI†). It was observed that an increase in excitation wavelength resulted in red-shifted PL emission (which is an intrinsic property of CNDs), as expected.[36] But the most intense emissions were observed at 365 and 425 nm photoexcitation. Fig. 4 shows normalised PL spectra of the CND–ORMOSIL film. It clearly shows that the light emitting property of the CNDs remained the same in the case of the CND–ORMOSIL films. The uniform and agglomeration-free distribution of CNDs in the film matrix observed in TEM

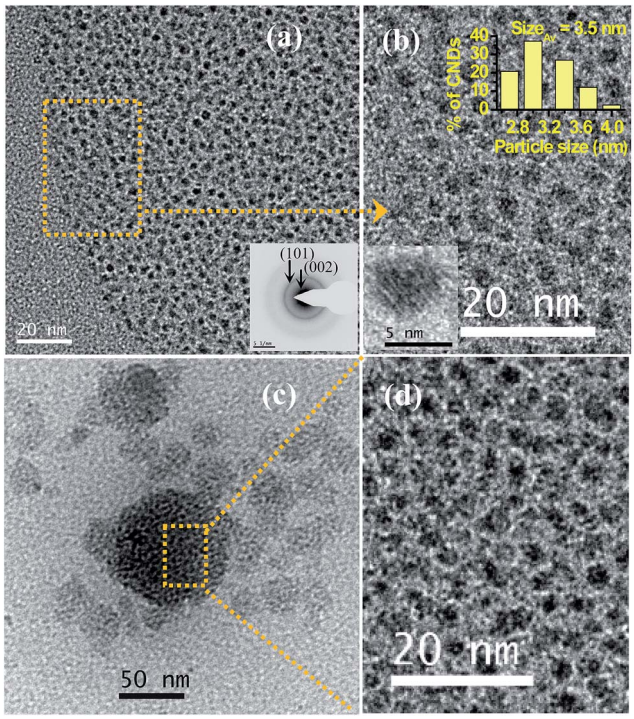

Fig. 3 (a and b) Bright field TEM images of purified CNDs at different magnifications, showing well dispersed CNDs. Insets in (a) and (b) show SAED patterns with faint rings corresponding to the (002) and (101) planes, and the size distribution of CNDs, respectively; (c and d) bright field TEM images of the CNDs in the ORMOSIL film at different magnifications. TEM shows that the solution-extracted CNDs and CNDs embedded in ORMOSIL are similar. In the case of the film, a scraped film sample was dispersed in methanol and used for TEM study (see Experimental, section 1.4 ESI†).

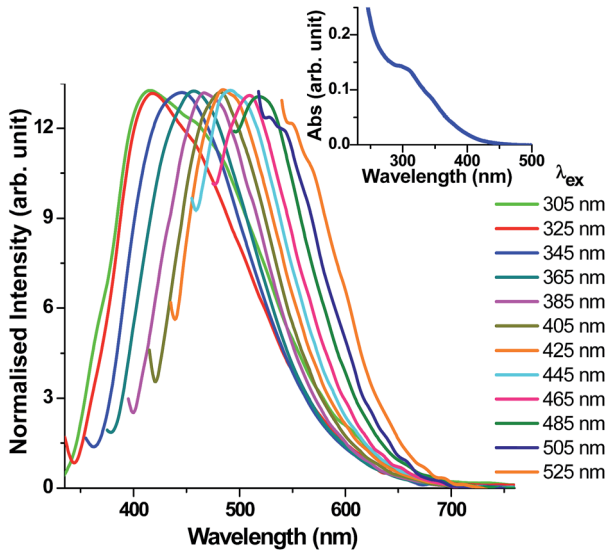

Fig. 4 PL spectra of the same CND–ORMOSIL film, showing the multicoloured emission when excited at different wavelengths. The inset shows the UV-visible absorption of the CND–ORMOSIL film.

analysis helped in understanding the reason behind the unaltered absorption and emission properties measured from UV-Vis and PL spectroscopy. A slight decrease in PL intensity was observed in the case of films due to the decrease in concentration of CNDs compared to the solution phase. Basically, PL emission in CNDs arises due to electronic transition from the highest σ-occupied molecular orbital (HOMO) to lowest unoccupied molecular orbital (LUMO). It is likely that different kinds of electronic transitions are expected to take place if a slight distribution of particle sizes is present.

Since smaller particles have a larger HOMO–LUMO gap than bigger particles, a bathochromic PL emission was observed with the increase in excitation wavelength (Fig. 5). A similar observation was made under a fluorescence microscope when CND–ORMOSIL coated on glass was illuminated with 3 different light sources. Fig. 6 shows the different coloured emissions (cyan, green, red) of the same film when excited with UV, blue and green light sources using band-pass filters of different wavelengths: 450, 550 and 580 nm, respectively. A relative quantum yield of the CNDs (in hexane) was measured against 10^{-4} M quinine sulfate (QY 58% in 0.01 N H_2SO_4 solution) as a standard[13] and found to be 10% (see Experimental, section 1.5 and Table S1; ESI†). This yield is quite high in comparison to the average values reported by others.[11,17,36–38] It should be noted here that the estimation of QY of CNDs, using rhodamine B[12,37] as a standard, can be erroneous. Since CNDs absorb in the wavelength region of 250–380 nm and rhodamine B at around 540 nm, selection of a common excitation wavelength for both CNDs and rhodamine B is always misleading, and a higher QY value can be obtained. So it is better to use a standard dye molecule, which absorbs in nearly the same absorption region as the QDs. As the absorption of quinine sulfate matches that of CNDs, we used this dye for QY calculation.[39] In this situation, the maximum emission of the dye molecules can be recorded and hence QY calculation will be more accurate. Fig. 7 shows the PL decay curves of CNDs (in hexane) and the CND–ORMOSIL film, measured at a 460 nm emission wavelength using a picosecond diode laser (λ = 375 nm). The average lifetime was calculated from tri-exponentially fitted curves and it was around 2.22 and 1.82 ns for CNDs (in hexane) and the CND–ORMOSIL film, respectively (Table S2; ESI†).

We observed that the films are quite photostable. Only about a 5% decrease in the PL intensity was observed when the films were stored for 30 days under ambient conditions

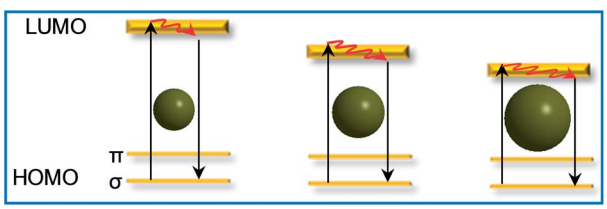

Fig. 5 Schematic diagram showing the decrease in HOMO–LUMO gap with increase in particle size of CNDs.

Fig. 6 Fluorescence images of the same CND-incorporated ORMOSIL film on a glass substrate (both sides coated) under different excitation sources (UV, blue and green; from left to right). The length of the scale bars shown in the figure is 0.2 mm. The photographs were taken in such a way that the layer of the opposite side is also visible.

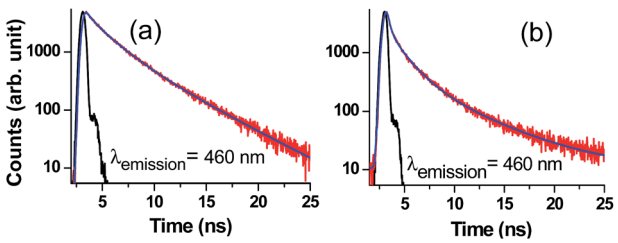

Fig. 7 Decay lifetime spectra of CNDs in hexane (a) and the CND–ORMOSIL film (b).

(Fig. S9; ESI†). As a representative application, we have tested the CND–ORMOSIL film as a UV-A absorbing filter. When a CND–ORMOSIL coating deposited on a 50 × 50 cm^2 glass substrate was irradiated with UV light sources of 310, 365 and 390 nm (8 W power; placed 2 cm away from the source), no noticeable power was observed using an UV power puck sensor (S/N-8000; EIT Inc.) placed 1 cm away on the opposite side of the film. However, a power of 7 mW cm^{-2} was observed when an undoped ORMOSIL film was irradiated with the same source. This suggests that the CND–ORMOSIL coatings on glass used for lamp fabrication can act as a UV-A radiation cut-off filter with emission of bright cyan light.

In conclusion, we have synthesised fluorescent CNDs from P123 block-*co*-polymer at room temperature and purified them from unwanted salts and excess P123. These dots are soluble in organic solvents (methanol, ethanol, DCM, *n*-hexane) and have relatively high QY (10%). A CND-incorporated ORMOSIL sol was used for the fabrication of scratch-resistant and highly fluorescent films on glass. Moreover, this kind of sol can be used as an eco-friendly fluorescent paint/ink. Eventually, this kind of coating could be used to make a fluorescent lamp that can completely cut off UV-A radiation and emit a visible cyan colour. The films can also be deposited on flexible plastics. This report will extend the use of fluorescent CNDs beyond the solution and powder phases.

Acknowledgements

The authors thank CSIR, India for support (project no. ESC 0202). MKM, AC and KB thank CSIR for awarding fellowships.

Notes and references

1 Q. Sun, Y. A. Wang, L. S. Li, D. Wang, T. Zhu, J. Xu, C. Yang and Y. Li, *Nat. Photonics*, 2007, **1**, 717.
2 S. T. Selvan, P. K. Patra, C. Y. Ang and J. Y. Ying, *Angew. Chem.*, 2007, **119**, 2500.
3 M. Green, H. Harwood, C. Barrowman, P. Rahman, A. Eggeman, F. Festry, P. Dobson and T. Ng, *J. Mater. Chem.*, 2007, **17**, 1989.
4 D. Bera, L. Qian, T. K. Tseng and P. H. Holloway, *Materials*, 2010, **3**, 2260.
5 L. Y. T. Chou and W. C. W. Chan, *Nat. Nanotechnol.*, 2012, **7**, 416.
6 A. M. Derfus, W. C. W. Chan and S. N. Bhatia, *Nano Lett.*, 2004, **4**, 11.
7 E. P. Painter, *Chem. Rev.*, 1941, **28**, 179.
8 M. W. Warenycia, L. R. Goodwin, C. G. Benishin, R. J. Reiffenstein, D. M. Francom, J. D. Taylor and F. P. Dieken, *Biochem. Pharmacol.*, 1989, **38**, 973.
9 B. B. Srivastava, S. Jana and N. Pradhan, *J. Am. Chem. Soc.*, 2011, **133**, 1007.
10 A. Nag, S. Chakraborty and D. D. Sarma, *J. Am. Chem. Soc.*, 2008, **130**, 10605.
11 Y. P. Sun, B. Zhou, Y. Lin, W. Wang, K. A. S. Fernando, P. Pathak, M. J. Meziani, B. A. Harruff, X. Wang, H. Wang, P. G. Luo, H. Yang, M. E. Kose, B. Chen, L. M. Veca and S. Y. Xie, *J. Am. Chem. Soc.*, 2006, **128**, 7756.
12 H. Li, X. He, Z. Kang, H. Huang, Y. Liu, J. Liu, S. Lian, C. H. A. Tsang, X. Yang and S. T. Lee, *Angew. Chem., Int. Ed.*, 2010, **49**, 4430.
13 S. K. Bhunia, A. Saha, A. R. Maity, S. C. Ray and N. R. Jana, *Sci. Rep.*, 2013, **3**, 1.
14 H. Li, Z. Kang, Y. Liu and S. T. Lee, *J. Mater. Chem.*, 2012, **22**, 24230.
15 C. Liu, P. Zhang, F. Tian, W. Li, F. Lib and W. Liu, *J. Mater. Chem.*, 2011, **21**, 13163.
16 S. Zhu, J. Zhang, C. Qiao, S. Tang, Y. Li, W. Yuan, B. Li, L. Tian, F. Liu, R. Hu, H. Gao, H. Wei, H. Zhang, H. Sun and B. Yang, *Chem. Commun.*, 2011, **47**, 6858.
17 H. Liu, T. Ye and C. Mao, *Angew. Chem., Int. Ed.*, 2007, **46**, 6473.
18 S. J. Yu, M. W. Kang, H. C. Chang, K. M. Chen and Y. C. Yu, *J. Am. Chem. Soc.*, 2005, **127**, 17604.
19 X. Li, S. Zhang, S. A. Kulinich, Y. Liu and H. Zeng, *Sci. Rep.*, 2014, **4**, 1.
20 M. S. Peresin, Y. Habibi, A. H. Vesterinen, O. J. Rojas, J. J. Pawlak and J. V. Seppala, *Biomacromolecules*, 2010, **11**, 2471.
21 B. L. Wang, K. F. Ren, H. Chang, J. L. Wang and J. Ji, *ACS Appl. Mater. Interfaces*, 2013, **5**, 4136.
22 A. R. Madaria, A. Kumar, F. N. Ishikawa and C. Zhou, *Nano Res.*, 2010, **3**, 564.
23 Y. Zhao, A. Sugunan, T. Schmidt, A. Fornara, M. S. Topraka and M. Muhammeda, *J. Mater. Chem. A*, 2014, **2**, 13270.
24 S. Zhu, Q. Meng, L. Wang, J. Zhang, Y. Song, H. Jin, K. Zhang, H. Sun, H. Wang and B. Wang, *Angew. Chem., Int. Ed.*, 2013, **52**, 3953.

25 S. Zhu, J. Zhang, Y. Song, G. Zhang, H. Zhang and B. Yang, *Chin. J. Chem.*, 2012, **70**, 2311.
26 S. K. Medda and G. De, *Ind. Eng. Chem. Res.*, 2009, **48**, 4326.
27 C. Lü and B. Yang, *J. Mater. Chem.*, 2009, **19**, 2884.
28 F. Wang, Z. Xie, H. Zhang, C. Y. Liu and Y. G. Zhang, *Adv. Funct. Mater.*, 2011, **21**, 1027.
29 It is to be noted here that if excess H_2SO_4 was used to complete carbonisation of P123, the CNDs formed were found to be unstable and slowly precipitated.
30 M. K. Mishra and G. De, *J. Mater. Chem. C*, 2013, **1**, 4816.
31 F. Quignard, R. Valentin and F. D. Renzo, *New J. Chem.*, 2008, **32**, 1300.
32 Z. Hu, Y. Chen, Q. Hou, R. Yin, F. Liu and H. Chen, *New J. Chem.*, 2012, **36**, 1373.
33 H. C. Schniepp, J. L. Li, M. J. M. Allister, H. Sai, M. H. Alonso, D. H. Adamson, R. K. Prudhomme, R. Car, D. A. Saville and I. A. Aksay, *J. Phys. Chem. B*, 2006, **110**, 8535.
34 L. Xu and L. Cheng, *J. Nanomater.*, 2013, **2013**, 731875, DOI: 10.1155/2013/731875.
35 K. N. Kudin, B. Ozbas, H. C. Schniepp, R. K. Prudhomme, I. A. Aksay and R. Car, *Nano Lett.*, 2008, **8**, 36.
36 M. P. Sk, A. Jaiswal, A. Paul, S. S. Ghosh and A. Chattopadhyay, *Sci. Rep.*, 2012, **2**, 1.
37 J. Shen, Y. Zhu, C. Chen, X. Yang and C. Li, *Chem. Commun.*, 2011, **47**, 2580.
38 A. B. Bourlinos, A. Stassinopoulos, D. Anglos, R. Zboril, M. Karakassides and E. P. Giannelis, *Small*, 2008, **4**, 455.
39 A. M. Brouwer, *Pure Appl. Chem.*, 2011, **83**, 2213.